

# Demagnetization of electrons in inhomogeneous $\mathbf{E} \perp \mathbf{B}$ : Implications for electron heating in shocks

M. Gedalin and K. Gedalin

Department of Physics, Ben-Gurion University, Beer-Sheva, Israel

M. Balikhin and V. Krasnoselskikh

Laboratoire de Physique et Chimie de l'Environnement, CNRS, Orleans, France

L.J.C. Woolliscroft

Department of Automatic Control and Systems Engineering, University of Sheffield, Sheffield, England

## 1. 1. Introduction

Collisionless shocks are one of the fundamental phenomena in plasmas in general and in space plasmas in particular. Collisionless shocks play an important role in many space and astrophysical systems, such as Wolf-Rayet stars, solar atmosphere, supernova remnants, astrophysical jets, and the planetary magnetosphere - solar wind interface etc. Electron heating is one of the most important problems of collisionless shock physics not only because in a number of cases it is the only direct indication of the shock presence (as in supernovae shocks [Drain and McKee, 1993]) but also because it is an important channel of the incoming bulk plasma flow energy redistribution, especially in interstellar shocks [Drain and McKee, 1993]. Thus it is related to shock formation and stability [Feldman, 1985]. While ions are relatively insensitive to the shock fine structure and behave essentially as if the shock was a jump of the magnetic field and electrostatic potential, electron dynamics depends significantly on the details of the shock structure. Measurements of the electron distribution function therefore provide indirect information about what happens in the shock at typical electron scales  $\sim c/\omega_{pe}$  and times  $\sim \Omega_e^{-1}$ . One has only to learn how the particle data can be translated into the electromagnetic field data.

During the last three decades of shock exploration in the heliosphere, a large body of data on electron heating in quasi-perpendicular shocks has been collected. Observations [Montgomery *et al.*, 1970; Feldman, 1985; Scudder *et al.*, 1986b] show that electron heating at quasiperpendicular shocks is prompt (the heating region is not resolved [Scudder *et al.*, 1986b]) and apparently takes place in the shock ramp, that is, the most narrow place of the shock front structure, where the magnetic field gradient is largest. The prevailing view now is that the heating is primarily due to the electron interaction with the reversible regular electromagnetic field, rather than to irreversible processes such as turbulent heating [Goodrich and Scudder, 1984; Feldman, 1985; Scudder *et al.*, 1986b; Thomsen *et al.*, 1987; Schwartz *et al.*, 1988]. The latter play an important role in the determination of the final distribution shape, but are of little importance in the energy transfer from ions to electrons. This conclusion is supported by numerical simulations [Veltri *et al.*, 1990; Liewer *et al.*, 1991; Veltri and Zimbardo, 1993].

It is usually believed that electrons are magnetized throughout the ramp, since the magnetic field variation scale is considerably larger than the electron gyroradius. Then the only mechanism of perpendicular heating is adiabatic heating  $T_{\perp} \propto B$ . If all heating was purely adiabatic, the downstream temperature would be  $T_{ad} = (2T_{\perp}(B_d/B_u) + T_{\parallel})/3$  ( $\perp$  and  $\parallel$  refer to the local magnetic field direction). Observations [Thomsen *et al.*, 1987; Schwartz *et al.*, 1988] showed that often the measured downstream temperature greatly exceeds the adiabatic value, which means that an additional (or alternative) mechanism exists that provides the required heating magnitudes.

Adiabatic electrons experience an acceleration along the magnetic field lines due to the parallel component of the electric field [Feldman, 1985]. As a result, at first a strongly accelerated electron beam forms, which is cooled in the parallel direction and weakly heated in the perpendicular direction. Eventual nearly isotropic downstream distribution forms due to irreversible processes at the second step, when the gap in the parallel degree of freedom is filled, and the accelerated beam energy is redistributed among all degrees of freedom. Strong pitch angle diffusion is required for the latter. Veltri and Zimbardo [1993] have shown that the redistribution of a modest ( $< 10\%$ ) energy excess requires that a rather high level of a proper turbulence be present and the heating region be much longer than the ramp width.

The gap can be filled by a preexisting electron population [Feldman, 1985] in which case the downstream temperature is not determined by the heating mechanism but by these preexisting electrons.

Electrons are assumed to be magnetized since the typical ramp width  $L_R$  is much larger than the electron gyroradius  $\rho_e$ . Numerical simulations of high Mach number perpendicular shocks [Tokar *et al.*, 1986] showed that electrons become demagnetized in this regime, since the ramp width becomes as small as an electron gyroradius. Galeev *et al.* [1988] proposed that electrons can become demagnetized even for moderate Mach number shocks with large  $\beta$ , when  $L_R \sim c/\omega_{pe} \sim \rho_e$ . Cole [1976] related breakdown of magnetization to the electric field inhomogeneity and showed that in  $B_z = \text{const}$  and steep  $E_x(x)$  electrons do not drift but are accelerated in  $x$  direction. Balikhin *et al.* [1989, 1993] generalized this analysis

onto the inhomogeneous  $\mathbf{B}$  case and applied it to the electron dynamics in the perpendicular shock front. Such nonadiabatic behavior occurs even when  $L_R \gg \rho_e$ .

*Gedalin et al.* [1995a, b] extended the analysis of *Balikhin et al.* [1993] to the oblique case and showed that the adiabaticity breaks down when  $\alpha = -(e/m_e \Omega^2)(dE_x/dx) > 0$  ( $x$  is along the shock normal and  $\Omega = eB/m_e$  is the local electron gyrofrequency). The energization, however, depends strongly on how large the nonadiabaticity parameter  $\alpha$  is. The resulting heating also depends on the initial electron temperature.

The breakdown of adiabaticity results in strong perpendicular heating, which is accompanied by corresponding parallel heating (in contrast with the adiabatic case in which the electrons are cooled in the parallel direction before irreversible processes start to work), and also in the substantial deceleration of the electron beam formed due to the acceleration along the magnetic field [*Gedalin*, 1994], in comparison to the adiabatic regime. The gap in the distribution is much smaller, and strong pitch angle diffusion is not necessary, so that the eventual distribution formation can be accomplished by nearly one-dimensional relaxation which is much faster [cf. *Veltri and Zimbardo*, 1993].

In the present paper we analyze in detail the electron motion in the perpendicular shock geometry and apply the analysis to the problem of the shock electron heating. We choose the perpendicular geometry in order to avoid mixing with Feldman's mechanism due to a parallel electric field and to show that the perpendicular heating features are due to the inhomogeneity of  $\mathbf{E} \perp \mathbf{B}$ . *Gedalin et al.* [1995a, b] have shown that if the adiabaticity is strongly broken, the electron motion along the electric field is the same in the oblique case as in the perpendicular case, at least when  $\alpha \gtrsim 1$  and the angle  $\theta$  between the shock normal and upstream magnetic field is large ( $\cos^2 \theta \ll 1$ ).

The paper is organized as follows. In section 2 we derive the expression for the cross-shock electric field in the perpendicular shock model in the framework of the two-fluid hydrodynamics. We discuss the observations of the ramp thickness and electric field, and numerical simulations as well. In section 3 we briefly describe the mechanism of demagnetization and heating in the steep electric field perpendicular to the external magnetic field. We discuss the observational evidence of the possible breakdown of adiabaticity. In section 4 we present numerical results and compare it to the existing experimental data.

## 2. 2. Electric Field

In the spirit of *Goodrich and Scudder* [1984] we assume that the shock is time-stationary, one-dimensional, and that the ramp width is between the typical ion and electron lengths. We start with the stationary one-dimensional two-fluid hydrodynamics in the perpendicular geometry. Let the shock normal (inhomogeneity direction) be along  $x$  axis, while the magnetic field be  $\mathbf{B} = [0, 0, B(x)]$ . The electric field  $\mathbf{E} = [E_x(x), E_y = \text{const}, 0]$ , where  $E_y = -V_u B_u$  (subscripts  $u$  and  $d$  refer to upstream and downstream, respectively). Since the problem is separable, we can restrict ourselves to  $x$  and  $y$  components only. Assuming quasi-neutrality  $n_e = n_i = n$  and  $v_{xe} = v_{xi} = v$ , one has

$$v \frac{dv}{dx} = \frac{e}{m_i} (E_x + v_{yi} B) - \frac{1}{nm_i} \frac{dp_i}{dx}, \quad (1)$$

$$v \frac{dv}{dx} - \frac{e}{m_e} (E_x + v_{ye} B) - \frac{1}{nm_e} \frac{dp_e}{dx}, \quad (2)$$

$$m_i v \frac{dv_{iy}}{dx} = e(E_y - vB) = -m_e v \frac{dv_{ey}}{dx}, \quad (3)$$

$$\frac{dB}{dx} = \mu_0 n e (v_{ey} - v_{iy}), \quad (4)$$

where  $\mu_0$  is the permeability of free space. Equation (3) shows that  $|v_{yi}/v_{ye}| = m_e/m_i \ll 1$  and that  $v_{yi}$  is negligible. Then (4) and (2) give

$$-eE_x = \frac{1}{2n\mu_0} \frac{dB^2}{dx} + \frac{1}{n} \frac{dp_e}{dx} + \frac{d}{dx} \left( \frac{m_e v^2}{2} \right), \quad (5)$$

We put  $m_e = 0$ , as usual, and use the widely accepted approximation  $n \propto B$ , which is well established at scales larger than the ramp width [*Scudder et al.*, 1986a].

The cross-ramp potential then takes the following form:

$$e\varphi = \frac{B_u^2(R-1)}{\mu_0 n_u} + \int \frac{1}{n} \frac{dp_e}{dx} dx, \quad (6)$$

where  $R = B_m/B_u$ , and  $u$  and  $m$  refer to the upstream and downstream sides of the ramp. The ratio  $O = B_m/B_d$ , where  $B_d$  is the true downstream magnetic field in the shock overshoot ( $d$  refers to downstream). According to *Mellott and Livesey* [1987],  $O \gtrsim 1.5$ . In dimensionless form one has

$$s = \frac{e\varphi}{\epsilon_i} = \frac{2(R-1)}{M^2} + \frac{e\varphi_p}{\epsilon_i}, \quad (7)$$

where  $\epsilon_i = m_i V_u^2 / 2$  is the the upstream ion energy,  $M$  is the upstream Alfvén Mach number, and  $e\varphi_p$  is the second term on the right-hand side of (6).

It is difficult to estimate the pressure-induced term  $e\varphi_p/\epsilon_i$  in (7) from first principles. We shall use the results of the statistical analysis by *Schwartz et al.* [1988], who applied the assumption  $p_e \propto n^\gamma$  and obtained

$$s_1 = \frac{e\varphi_p}{\epsilon_i} = \frac{\gamma}{\gamma - 1} \frac{T_d - T_u}{\epsilon_i} \approx 0.1 - 0.3, \quad (8)$$

In the oblique case the expression for the electric field is more complicated (see, for example, *Scudder et al.* [1986b]), partly due to the presence of the noncoplanar component of the magnetic field. However, the same approximate expression (6) is widely used in the assumption of the pressure isotropy [*Schwartz et al.*, 1988]. In the gyrotropic case  $p_{\parallel} \neq p_{\perp}$  one should substitute  $p \rightarrow p_{\perp}$  in (6), in the quasi-perpendicular regime  $\cos^2 \theta \ll 1$ . The term  $e\varphi_p$  is the de Hoffman-Teller cross-shock potential, which is the net electron energy budget [*Goodrich and Scudder*, 1984] and is directly related to the perpendicular electron heating. This relation, together with the observation that the heating region is not resolved and is not wider than the ramp [*Scudder et al.*, 1986b], lead to the conclusion that the heating occurs inside the ramp and the de Hoffman-Teller potential drop is applied at the ramp.

The available observational electric field data is rather poor. In the only comprehensively documented supercritical shock by *Scudder et al.* [1986a, b] the spatial separation between the two successive electric field measurements is larger than the ramp width itself. The averaging interval for the particle data is also greater than the ramp width, which does not allow to deduce the fine scale profile of the electric field. *Scudder et al.* [1986a, b] found the normal incidence frame (NIF, where  $\mathbf{V}_u$  is parallel to the shock normal) cross-shock potential drop to be  $s \approx 0.9$ , while the de Hoffman-Teller potential drop  $s_1 \approx 0.1$ . Poor resolution does not allow to conclude what fraction of the total potential drop is applied at the ramp. The value of  $s_1$  is rather small [cf. *Schwartz et al.*, 1988]. It should be noted that the shock, described by *Scudder et al.* [1986a,b], exhibits only weak electron heating and its features may differ greatly from the features of the shocks, in which electron heating is strong.

High-resolution electric field measurements show that there exist large dc electric fields inside the ramp [*Heppner et al.*, 1978], probably with the scales down to  $c/\omega_{pe}$ , and that most of the cross-shock potential is applied at the ramp itself [*Wygant et al.*, 1987], with a large electric field peak just in the middle of the ramp.

Hybrid simulations also give the NIF cross-shock potential drop of  $s \approx 0.6 - 0.8$  [*Goodrich*, 1985]. These simulations also show that this potential drop decreases with the increase of the Mach number, which is in an agreement with (7). The field scales, however, are lost due to the treatment of electrons as a massless fluid. *Liewer et al.* [1991] found in one-dimensional full particle simulations with  $m_i/m_e = 1600$  that the main potential drop is applied at the ramp and the electron heating is associated with the inhomogeneous  $\mathbf{E} \perp \mathbf{B}$ .

So far there is no good theory which would provide a reliable estimate for the ramp width. *Scudder et al.* [1986a] found that the ramp width is  $4 \text{ km} < L_R < 21 \text{ km}$ , while  $c/\omega_{pe} = 1.7 \text{ km}$ , that is,  $2.5(c/\omega_{pe}) < L_R < 12(c/\omega_{pe})$ , with the best estimate  $L_R \approx 8(c/\omega_{pe})$ . Analysis of subcritical shocks shows that the ramp width is of  $(1 - 2)l_W$ , where  $l_W = 2\pi c \cos \theta / \omega_{pi} (M^2 - 1)^{1/2}$  is the whistler precursor length [*Mellott and Greenstadt*, 1984; *Farris et al.*, 1993]. The ramp width of the perpendicular shocks is believed to be of the order of  $c/\omega_{pe}$  [*Kennel et al.*, 1985]. *Newbury and Russell* [1994] reported a highly quasi-perpendicular  $\theta \approx 85$  deg supercritical shock with the ramp width of  $\approx 2(c/\omega_{pe})$ . In what follows we therefore assume that the ramp width of the perpendicular shock is several electron inertial lengths and use the approximation (7).

### 3. 3. Electron Demagnetization and Heating Mechanism

The nonadiabatic mechanism has been described in details by *Balikhin et al.* [1993] and *Gedalin et al.* [1995a, b]. Here we briefly describe the basic features.

The equations of motion for an electron in the general oblique shock geometry (shock normal is along  $x$ ) are

$$m_e \dot{v}_x = -e(E_x + v_y B_z - v_z B_y), \quad (9)$$

$$m_e \dot{v}_y = -e(E_y + v_z B_x - v_x B_z), \quad (10)$$

$$m_e \dot{v}_z = -e(v_x B_y - v_y B_x), \quad (11)$$

where we have taken into account that  $E_z = 0$ . Let us assume for simplicity that  $\mathbf{B} = \text{const}$  and  $dE_x/dx = \text{const}$ . Then differentiating (9) with respect to time and using  $dE_x/dt = (dE_x/dx)v_x$  one has

$$m_e \ddot{v}_x = -e \left( \frac{dE_x}{dx} v_x + \dot{v}_y B_z - \dot{v}_z B_y \right). \quad (12)$$

For  $E_y = \text{const}$ , a general solution of the form [*Gedalin et al.*, 1995b]

$$v_x = \sum_i^4 A_i \exp(\lambda_i \Omega t), \quad (13)$$

is obtained, where  $\Omega = eB/m_e$  and  $B^2 = B_x^2 + B_y^2 + B_z^2$ . The exponents  $\lambda_i$  are the four roots of

$$\lambda^4 + \lambda^2(1 - \alpha) + \alpha \cos^2 \theta = 0, \quad (14)$$

and  $\cos \theta = B_x/B$ . The nonadiabaticity parameter  $\alpha$  is defined as

$$\alpha = -\frac{e}{m_e \Omega^2} \frac{dE_x}{dx}. \quad (15)$$

In the case  $\alpha < 0$  one has  $\lambda^2 < 0$ , and all  $\lambda_i$  are purely imaginary, which corresponds to the electron gyration about the magnetic field. However, if  $\alpha > 0$  one of the roots becomes real and positive, so that the gyration changes to a runaway along the  $E_x$  electric field. The electron is accelerated along the shock normal, and there is energy input into the perpendicular degree of freedom. In a finite spatial region, like a ramp, where the adiabaticity can be broken only partially, adiabaticity is restored eventually, and all acquired energy goes directly into electron gyration energy. The perpendicular energy, acquired by an electron, can constitute a substantial part of the cross-shock potential, and it depends strongly on the initial electron velocity [Balikhin *et al.*, 1993; Gedalin *et al.*, 1995b]. For an initially cool distribution this mechanism would result in a rather large spread in the perpendicular energy space in the downstream distribution, which is measured as a perpendicular temperature.

This breakdown of adiabaticity occurs in the oblique case when  $\alpha > 0$ . The resulting energization, however, depends strongly on  $\alpha$  and becomes large if  $\alpha \sim 1$  (in the oblique case).

In the perpendicular regime  $\cos \theta = 0$  and the demagnetization condition reads  $\alpha > 1$ . It is easy to see that well above this threshold one has to retain only the largest  $\lambda$  term in (13), so that motion features in the oblique case and in the perpendicular case should be alike for the strongly nonadiabatic case [cf. Gedalin *et al.*, 1995b].

Whether the adiabaticity can be strongly broken in a real shock front depends on the shock parameters. Let us define the ramp half-width  $D$  measured in the electron inertial lengths  $c/\omega_{pe}$ . Then for a single-peaked electric field with a triangle profile in the ramp  $dE_x/dx \approx \varphi/[D^2(c/\omega_{pe})^2]$  and the nonadiabaticity parameter

$$\alpha \approx \frac{M^2 s}{2D^2} \gtrsim \frac{R-1}{D^2}, \quad (16)$$

the inequality  $(R-1)/D^2 \gtrsim 1$  can be considered as a rough approximation of the strong adiabaticity condition. Applying it to the shock described by Scudder *et al.* [1986a], where  $M = 7.7$ ,  $R = 6$  (at the ramp!), and  $s_1 \approx 0.1$  [Scudder *et al.*, 1986b], one has  $s \approx 0.27$ , and for  $D \approx 4$  one obtains  $\alpha \approx 0.5$ , which is moderately nonadiabatic in the oblique case. In agreement with this estimate the shock described by Scudder *et al.* [1986a] exhibits only slightly overadiabatic heating.

It should be understood that the demagnetization criterion, obtained from (14), is only a simple approximation. Actual breakdown of adiabaticity is trajectory dependent, which causes smearing out of the condition  $\alpha > 1$  [Balikhin *et al.*, 1993]. We shall use the condition  $\alpha > 1$  as an indication of the dramatic influence of the demagnetization on the electron heating.

#### 4. 4. Numerical Analysis and Comparison With Observations

In this section we carry out a numerical analysis of the electron motion for a model structure of the perpendicular shock ramp. The choice of the perpendicular geometry allows to avoid the complications, related to the noncoplanar component of the magnetic field, and also allows us to distinguish between the effects due to parallel and perpendicular electric field components. At the same time this choice greatly reduces the necessary computation time, which is important for statistical analysis. The perpendicular case is stiff relative to the oblique one, in the sense that nonadiabaticity strictly requires  $\alpha > 1$ . However, in the limit of strong nonadiabaticity, the motion along the shock normal is almost the same in both cases. Hence we expect that qualitative features of the heating (for example, correlation with the shock parameters) will be similar.

We specify the magnetic field in the model ramp according to the following requirements: (1) it should resemble the actual ramp structure, (2) its second derivative should be conservative, and (3) it should be a polynomial of the lowest possible order. These requirements lead to the following choice:

$$\frac{B_z}{B_u} = \frac{R+1}{2} + \frac{R-1}{16} \left[ 3\left(\frac{x}{l}\right)^5 - 10\left(\frac{x}{l}\right)^3 + 15\left(\frac{x}{l}\right) \right] \quad (17)$$

inside the ramp  $-l < x < l$ ,  $l = D(c/\omega_{pe})$ , and  $B = B_u$  at  $x < -l$ ,  $B = RB_u$  at  $x > l$ .

The model electric field is taken in the form

$$E_x = -\frac{sB_u}{en_u \mu_0} \frac{dB}{dx}, \quad (18)$$

where

$$s = \frac{2(R-1)}{M^2} + s_1. \quad (19)$$

It should be emphasized that the cross-ramp potential drop is only a part of the observed cross-shock potential drop, which extends to the upstream and downstream region over the scale much larger than the ramp width. The breakdown of adiabaticity occurs only inside the ramp, therefore we do not have to take into account the extended part of the potential, which is responsible only for the additional slow  $\mathbf{E} \times \mathbf{B}$  drift.

The dimensionless parameters  $M$  (Mach number),  $R$  (magnetic compression ratio at the ramp),  $D$  (ramp half width), and  $s_1$  (pressure-induced potential) are the model input parameters. The initial electron distribution is described by  $v_h = v_T/V_u$  (upstream electron thermal velocity / upstream bulk plasma velocity).

The model shock structure used in the numerical analysis is shown in Figure 1 for the following set of parameters:

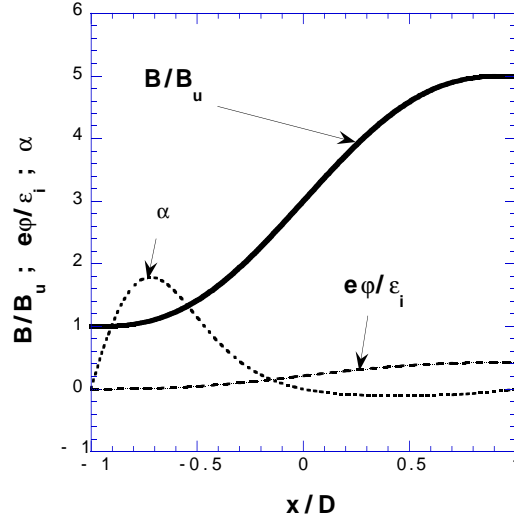


**Figure 1.** Model ramp structure in the case  $M = 5$ ,  $R = 5$ ,  $D = 2$ , and  $s_1 = 0.2$ .

$M = 5$ ,  $R = 5$ ,  $D = 2$ , and  $s_1 = 0.2$ . The nonadiabaticity parameter  $\alpha$  is shown inside the ramp together with the dimensionless magnetic field  $B(x)/B_u$  and dimensionless cross-shock potential  $\varphi(x)/(m_i V_u^2/2e)$ .

Figure 2 shows a typical electron trajectory  $v_x(x)$  in the nonadiabatic regime. The initial electron conditions are  $x(0)$

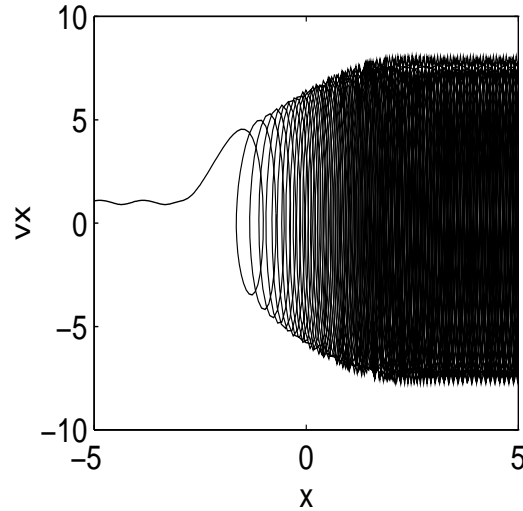


**Figure 2.** Typical electron trajectory  $v_x(x)$  in the nonadiabatic case  $M = 7$ ,  $R = 6$ ,  $s_1 = 0.15$ , and  $D = 3$ .

$= -10(c/\omega_{pe})$ ,  $v_x(0) = V_u + v_{\perp 0}$ ,  $v_y(0) = 0$ , where  $v_{\perp 0} = 0.1 V_u$ , and  $V_u$  is the upstream bulk plasma velocity. The input parameters are chosen as follows:  $M = 7$ ,  $R = 6$ ,  $s_1 = 0.15$  and  $D = 3$ . For  $V_u = 400$  km/s and  $B_u = 5$  nT our choice corresponds to  $n \approx 3.7 \text{ cm}^{-3}$ ,  $c/\omega_{pe} \approx 2.8$  km, and the ramp width  $L_R = 2D(c/\omega_{pe}) \approx 16.8$  km. The corresponding nonadiabaticity parameter estimated according to (16) is  $\alpha \approx 0.96$ . The actual  $\alpha$  calculated from (15) is substantially larger  $\alpha_{max} \approx 1.3$ . The motion is clearly nonadiabatic and the electron acquires a large gyration energy. As is clearly seen from Figure 2, the electron is accelerated along the shock normal at the upstream edge of the ramp, where the adiabaticity is broken. The efficiency of the energization is described by the ratio of the energy increase to the upstream ion energy

$h_t = \Delta\epsilon_{\perp}/\epsilon_i = 0.03$  in the present case. Overadiabaticity is described by  $h_o = \epsilon_{\perp d}/\epsilon_{ad} \approx 500$ , where  $\epsilon_{\perp d} \approx 15 \text{ eV}$  is the calculated electron downstream energy and  $\epsilon_{ad} = R(m_e v_{\perp 0}^2/2) \approx 0.03 \text{ eV}$  in our case.

For the heating analysis an initial Maxwellian distribution for 1000 particles was traced from far upstream to far downstream region. The two-dimensional downstream distribution was constructed using the staying time method [Veltri *et al.*, 1990; Veltri and Zimbardo, 1993] by averaging over the layer  $15(c/\omega_{pe}) < x < 18(c/\omega_{pe})$ . We do not follow the  $y$  coordinate since the stationary shock is invariant with respect to the translations in  $y$  direction. Therefore, in the averaging layer all particles with the same initial  $y$  and different final  $y$  are counted. This is the same (but much easier technically) than to count particles with different initial  $y$  arriving at the same downstream point  $(x, y)$ . The perpendicular downstream temperature was calculated as

$$T_{\perp d} = \frac{m}{2} \langle (\mathbf{v}_{\perp} - \langle \mathbf{v}_{\perp} \rangle)^2 \rangle, \quad (20)$$

where  $\langle \dots \rangle$  denotes the average over the downstream distribution. The parallel temperature does not change.

A typical two-dimensional downstream distribution for the strongly nonadiabatic regime is shown in Figure 3. We

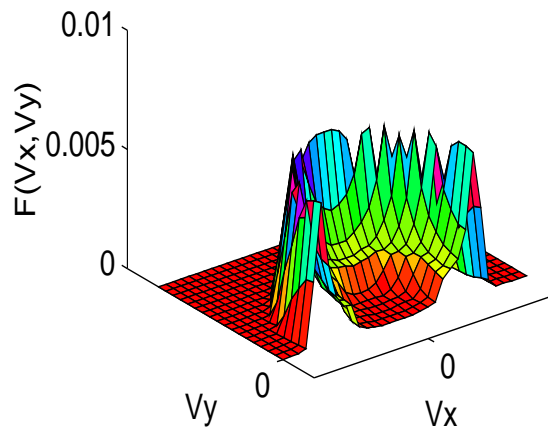


**Figure 3.** Typical two-dimensional downstream distribution  $f(v_x, v_y)$  in the nonadiabatic case  $M = 5$ ,  $R = 6$ ,  $s_1 = 0.2$ , and  $D = 2$ . The upstream coldness  $v_c = V_u/v_T = 0.43$ .

present a half of the distribution function  $f(v_x, v_y)$  cut along  $v_y = 0$ , in the velocity space  $(v_x, v_y)$ , perpendicular to the magnetic field. The input parameters are chosen as follows:  $V_u = 400 \text{ km/s}$ ,  $B_u = 10 \text{ nT}$ ,  $M = 5$ ,  $R = 6$ , and  $s_1 = 0.2$ , which corresponds to the cross-ramp potential  $\varphi = 0.6\epsilon_i = 500 \text{ V}$ . The upstream electron temperature is chosen as  $T_u = 5 \text{ eV} = 0.56 \cdot 10^5 \text{ K}$ , which corresponds to the coldness  $v_c = V_u/v_T = 0.43$ . The dimensionless ramp half width  $D = 2$ , which corresponds to the ramp width  $L_R \approx 7.7 \text{ km}$ .

The downstream distribution is clearly non-Maxwellian. As a result of the adiabaticity breakdown the electrons from the core of the initial distribution are strongly energized and form an energetic ring in velocity space. The high-energy tail of the initial Maxwellian is energized adiabatically. In Figure 4 the distribution function  $F(v_x) = \int f(v_x, v_y) dv_y$  is shown on a logarithmic scale. The form of the distribution resembles a flattop distribution [Feldman, 1985].

It is natural to describe the heating in dimensionless variables [Schwartz *et al.*, 1988]. For this purpose we use the perpendicular heating efficiency  $H_p = (T_{\perp d} - T_u)/\epsilon_i$  and the overadiabaticity  $H_o = T_{\perp d}/RT_u$ . In this present case  $H_p = 0.2$  and  $H_o = 3.7$ .

For the statistical analysis we use the same dimensionless variables taking the coldness  $v_c = V_u/v_T$  as an input parameter.

We performed the numerical calculations for four different ramp half widths:  $D = 1.5, 2, 3$ , and  $4$ . In each case the other parameters were the following: Mach number  $M = 5$ , and  $6$ ; magnetic compression ratio  $R = 5$ , and  $6$ ; and pressure-induced potential  $s_1 = 0.15, 0.2$ , and  $0.25$ . The coldness parameter varied in the range  $0.1 < V_u/v_T < 0.7$ . The results of the analysis are shown in Figures 5 and 6 in comparison with the observations. Solid circles correspond to the observational data. The elaborated data set is taken from Schwartz *et al.* [1988] (courtesy Steve Schwartz). This data has been collected during the ISEE 1 and 2 mission in 1977 – 1978 (78 Earth bow shock crossings) and two other planetary bow shock crossings (at Jupiter and Saturn). Only part of the data is shown, for which  $v_c > 0.1$ , since the rest of the data is deeply inside the adiabatic range of parameters. Crosses, triangles, open circles, and squares correspond to  $D = 1.5, 2, 3$ ,

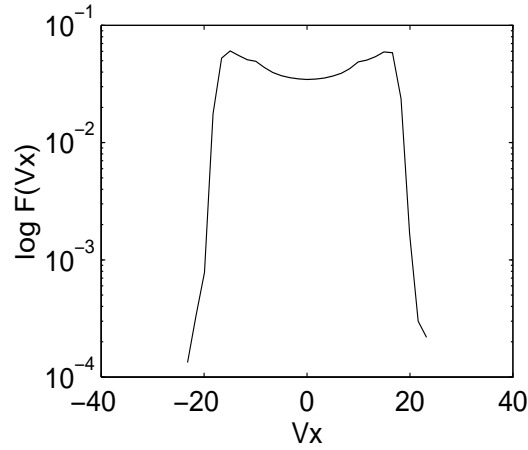


**Figure 4.** Integrated two-dimensional downstream distribution  $F(v_x) = \int f(v_x, v_y) dv_y$  in the nonadiabatic case (same as for Figure 3).

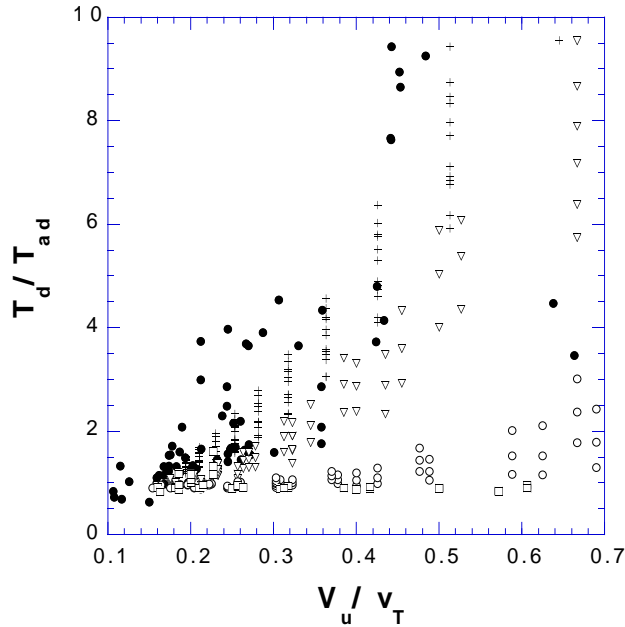


**Figure 5.** Overradiaticity  $T_d/RT_u$  versus upstream electron coldness  $V_u/v_T$ . Solid circles correspond to observations (data set from Schwartz *et al.* [1988], courtesy S. Schwartz). Crosses, triangles, open circles, and squares correspond to  $D = 1.5, 2, 3,$  and  $4,$  respectively.

and 4, respectively. The case  $D = 4$  corresponds to the adiabatic or almost adiabatic regime. The case  $D = 3$  corresponds to almost adiabatic or weakly adiabatic regimes. The cases  $D = 2$  and  $D = 1.5$  correspond to strong nonadiabaticity.

In Figure 5 the distribution of the overradiaticity  $H_o = T_{\perp d}/RT_u$  versus coldness  $v_c = V_u/v_T$  is shown. One can see that both observations and numerical analysis show rapid decrease of the overradiaticity with the decrease of the upstream electron coldness. The agreement between the observational and numerical values is quite good, if we take into account rather large observational uncertainties (S. Schwartz, private communication, 1994). One should remember also, that in real shocks the ramp width is a function of the shock parameters, while we treat it as an independent variable. Therefore not all of the parameter combinations used in the numerical model are realized in nature. On the other hand, our parameter range may not cover all available states of real shocks.

To compare the perpendicular heating efficiency with the observations, we have to take into account that the calculated  $H_p$  is achieved at the downstream edge of the ramp. The true downstream magnetic field obeys  $B_d < B_m$ , where  $B_m$  is the

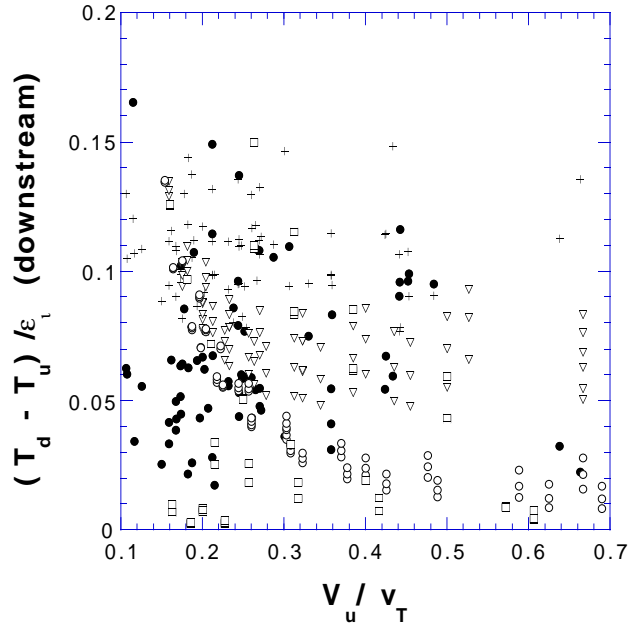


**Figure 6.** Heating efficiency  $(T_d - T_u)/\epsilon_{\perp}$  versus upstream electron coldness  $V_u/v_T$ . Solid circles correspond to observations (data set from *Schwartz et al.* [1988], courtesy S. Schwartz). Crosses, triangles, open circles, and squares correspond to  $D = 1.5, 2, 3,$  and  $4,$  respectively.

magnetic field at the downstream edge of the ramp (see section 2). Since in the downstream region electrons are completely magnetized,  $T_{\perp} \propto B$  and the true downstream perpendicular temperature  $T_{\perp dt} = T_u H_o R / O$ , where  $O = B_m / B_d$  (see section 2). The true downstream perpendicular heating efficiency is

$$H_{pt} = H_p \frac{H_o R / O - 1}{H_o R - 1}, \quad (21)$$

while the overadiabaticity  $H_o$  remains unchanged.

The true efficiency  $H_{pt}$  is presented in Figure 6 for  $O = 1.5$  [*Mellott and Livesey*, 1987] together with the observational data (the data set and marks are the same). Again good agreement with the observations can be seen.

It should be emphasized that a comparison in Figure 6 is done between the numerically-obtained perpendicular downstream temperature and observationally-determined perpendicular downstream temperature. The latter coincides with the overall downstream temperature due to the approximate isotropy of the observed distributions. In this connection, Figure 5 requires additional comments. Since the parallel temperature does not change in the strictly perpendicular case (it is not so in the oblique case, see section 5), the true three-dimensional downstream temperature is  $T_d = (T_u + 2T_{\perp d})/3 = T_u(1 + 2RH_o/O)/3$ . The corresponding adiabatic temperature is  $T_{ad} = T_u(1 + 2R/O)/3$ , so that the true three-dimensional overadiabaticity is

$$H_{ot} = \frac{1 + 2RH_o/O}{1 + 2R/O}. \quad (22)$$

For  $R/O > 3$  and  $H_o < 10$  one has  $(H_o - H_{ot})/H_o < 0.15$ . It is thus not very illuminating to substitute  $H_o$  for  $H_{ot}$  in Figure 5.

In the quasi-perpendicular case the strong perpendicular heating results in immediate parallel heating [*Gedalin et al.*, 1995a] and the above expression underestimates the resulting overadiabaticity.

## 5. 5. Discussion and Conclusions

The results obtained above for the perpendicular case can be extrapolated to the oblique case with caution. The strong nonadiabaticity condition in the oblique case  $\alpha \gtrsim 1$  is weaker than the corresponding condition  $\alpha > 1$  in the perpendicular case. Therefore, when  $\alpha \approx 1$  the two cases may differ significantly. Well above the threshold  $\alpha = 1$  the heating features can be expected to be similar in both cases. This has been confirmed in a single particle analysis [*Gedalin et al.*, 1995b] and in the analysis of the downstream distribution, which is formed in the quasi-perpendicular nonadiabatic case [*Gedalin et al.*, 1995a].

There is no parallel heating in the strictly perpendicular case, and the three-dimensional distribution becomes strongly anisotropic  $T_{\perp} \gg T_{\parallel}$ . In the quasi-perpendicular case  $1 \gg \cos \theta > (m_e/m_i)^{1/2}$  the situation is quite different, since the energy conservation in the de Hoffman-Teller frame [Goodrich and Scudder, 1984] imposes the condition  $\Delta\epsilon_{\perp} + \Delta\epsilon_{\parallel} = e\varphi^{HT} = \text{const}$ . Therefore, the energy spread in the perpendicular direction immediately results in a corresponding energy spread in the parallel direction, and the electrons are strongly heated in both directions. Still, anisotropy in favor of the perpendicular degree of freedom persists [Gedalin et al., 1995a], and a second irreversible step is needed to form the eventual nearly isotropic distribution. In this case, however, fast one-dimensional relaxation would efficiently isotropize the distribution [Veltri and Zimbardo, 1993]. On the other hand, deceleration of the electron beam in the nonadiabatic case (in comparison with the adiabatic regime) may solve the problem of the overly high parallel electron velocity observed in the simulations in the adiabatic regime [Veltri and Zimbardo, 1993]. More detailed analysis of the formation of the downstream distribution due to irreversible processes is beyond the scope of the present paper.

To conclude, we have considered nonadiabatic heating in a perpendicular shock geometry. This allowed us to show that the strong perpendicular heating is related to the inhomogeneous  $\mathbf{E} \perp \mathbf{B}$  in the shock front. We have shown that the heating efficiency depends strongly on the electric field profile and the initial electron temperature. Statistical analysis of the heating showed qualitative agreement of the numerically found correlations with those observed. It is suggested that the results can be qualitatively extrapolated onto quasi-perpendicular shocks in the strongly nonadiabatic regime.

#### Acknowledgments.

M. Balikhin and M. Gedalin are very grateful to S. Schwartz, C.T. Russell, and J.D. Scudder for useful and stimulating discussions. The authors are very grateful to S.J. Schwartz for the elaborated data. M. Gedalin is very grateful to W. Peter for the help in the preparation of the paper.

The Editor thanks C.T. Russell, V. Shapiro, and another referee for their assistance in evaluating this paper.

## References

- Balikhin, M., and M. Gedalin, Kinematic mechanism of electron heating in shocks: Theory versus observations, *Geophys. Res. Lett.*, , 21, 841, 1994.
- Balikhin, M.A., M.E. Gedalin, and J.G. Lominadze, A possible mechanism of electron heating in collisionless perpendicular shock front, *Adv. Space Res.*, 9, 135, 1989.
- Balikhin, M., M. Gedalin, and A. Petrukovich, New mechanism for electron heating in shocks, *Phys. Rev. Lett.*, , 70, 1259, 1993.
- Cole, K.D., Effects of crossed magnetic and (spatially dependent) electric fields on charged particle motion, *Planet. Space Sci.*, 24, 518, 1976.
- Drain, B.T., and C.F. McKee, Theory of interstellar shocks, *Ann. Rev. Astron. Astrophys.*, 31, 373, 1993.
- Farris, M.H., C.T. Russell, and M.F. Thomsen, Magnetic structure of the low beta, quasi-perpendicular shock, *J. Geophys. Res.*, , 98, 15,285, 1993.
- Feldman, W.C., Electron velocity distributions near collisionless shocks, in *Collisionless Shocks in the Heliosphere: Reviews of Current Research*, *Geophys. Monogr. Ser.*, vol. 35, edited by R.G. Stone and B.T. Tsurutani, p.195, AGU, Washington, D. C., 1985.
- Galeev, A.A., V.V. Krasnoselskikh, and V.V. Lobzin, Fine structure of the front of a quasiperpendicular supercritical collisionless shock wave, *Sov. J. Plasma Phys.*, 14, 697, 1988.
- Gedalin, M., Electron heating at shocks: Dependence on the shock width, *Eos Trans. AGU*, 75(44), Fall Meet.Suppl., 549, 1994.
- Gedalin, M., M. Balikhin, and V. Krasnoselskikh, Electron heating in collisionless shocks, *Adv. Space Res.*, 15(8/9), 225, 1995a.
- Gedalin, M., K. Gedalin, M. Balikhin, and V. Krasnoselskikh, Demagnetization of electrons in the electromagnetic field structure, typical for quasiperpendicular collisionless shock front, *J. Geophys. Res.*, , 100, 9481, 1995b.
- Goodrich, C.C., Numerical simulations of quasi-perpendicular collisionless shocks, in *Collisionless Shocks in the Heliosphere: Reviews of Current Research*, *Geophys. Monogr. Ser.*, vol. 35, edited by R.G. Stone and B.T. Tsurutani, p.153, AGU, Washington, D. C., 1985.
- Goodrich, C.C., and J.D. Scudder, The adiabatic energy change of plasma electrons and the frame dependence of the cross shock potential at collisionless magnetosonic shock waves, *J. Geophys. Res.*, , 89, 6654, 1984.
- Heppner, J.P., N.C. Maynard, and T.L. Aggson, Early results from ISEE-1 electric field measurements, *Sp. Sci. Rev.*, 22, 777, 1978.
- Kennel, C.F., J.P. Edmiston, and T. Hada, A quarter century of collisionless shock research, in *Collisionless Shocks in the Heliosphere: A Tutorial Review*, *Geophys. Monogr. Ser.*, vol. 34, edited by R.G. Stone and B.T. Tsurutani, pp. 1-36, AGU, Washington, D.C., 1985.
- Liewer, P.C., V.K. Decyk, J.M. Dawson, and N. Lembège, Numerical studies of electron dynamics in oblique quasi-perpendicular collisionless shock waves, *J. Geophys. Res.*, , 96, 9455, 1991.
- Mellott, M.M., and E.W. Greenstadt, The structure of oblique subcritical bow shocks: ISEE 1 and 2 observations, *J. Geophys. Res.*, 89, 2151, 1984.
- Mellott, M.M., and W.A. Livesey, Shock overshoots revisited, *J. Geophys. Res.*, , 92, 13,661, 1987.
- Montgomery, M.D., J.R. Asbridge, and S.J. Bame, Vela 4 plasma observations near the Earth's bow shock, *J. Geophys. Res.*, , 75, 1217, 1970.
- Newbury, J.A., and C.T. Russell, Observations of a very thin collisionless shock, *Eos Trans. AGU*, 75(44), Fall Meet.Suppl., 533, 1994.
- Schwartz, S.J., M.F. Thomsen, S.J. Bame, and J. Stansbury, Electron heating and the potential jump across fast mode shocks, *J. Geophys. Res.*, , 93, 12,923, 1988.
- Scudder, J.D., A. Mangeney, C. Lacombe, C.C. Harvey, T.L. Aggson, R.R. Anderson, J.T. Gosling, G. Paschmann, and C.T. Russell, The resolved layer of a collisionless, high  $\beta$ , supercritical, quasi-perpendicular shock wave, 1, Rankine-Hugoniot geometry, currents, and stationarity, *J. Geophys. Res.*, , 91, 11,019, 1986a.
- Scudder, J.D., A. Mangeney, C. Lacombe, C.C. Harvey, and T.L. Aggson, The resolved layer of a collisionless, high  $\beta$ , supercritical, quasi-perpendicular shock wave, 2, Dissipative fluid electrodynamics, and stationarity, *J. Geophys. Res.*, , 91, 11,053, 1986b.
- Thomsen, M.F., M.M. Mellott, J.A. Stansbury, S.J. Bame, J.T. Gosling, and C.T. Russell, Strong electron heating at the Earth's bow shock, *J. Geophys. Res.*, , 92, 10,119, 1987.
- Tokar, R.L., C.H. Aldrich, D.W. Forslund, and K.B. Quest, Nonadiabatic electron heating at high-Mach number perpendicular shocks, *Phys. Rev. Lett.*, , 56, 1059, 1986.
- Veltri, P., and G. Zimbardo, Electron - whistler interaction at the Earth's bow shock: 2, Electron pitch angle diffusion, *J. Geophys. Res.*, , 98, 13,335, 1993.
- Veltri, P., A. Mangeney, and J.D. Scudder, Electron heating in quasiperpendicular shocks: A Monte-Carlo simulation, *J. Geophys. Res.*, , 95, 14,939, 1990.
- Wygant, J.R., M. Bensadoun, and F.C. Mozer, Electric field measurements at subcritical, oblique bow shock crossings, *J. Geophys. Res.*, , 92, 11,109, 1987.